

Structural Disorder and Elementary Magnetic Properties of Triangular Lattice ErMgGaO₄

Single Crystals

F. Alex Cevallos, Karoline Stolze, and Robert J. Cava

Department of Chemistry, Princeton University, Princeton NJ 08544 USA

*Corresponding author: fac2@princeton.edu (F. Alex Cevallos)

Abstract

The single crystal growth, structure, and basic magnetic properties of ErMgGaO₄ are reported. The structure consists of triangular layers of magnetic ErO₆ octahedra separated by a double layer of randomly occupied non-magnetic (Ga,Mg)O₅ bipyramids. The Er atoms are positionally disordered. Magnetic measurements parallel and perpendicular to the *c* axis of a single crystal reveal dominantly antiferromagnetic interactions, with a small degree of magnetic anisotropy. A weighted average of the directional data suggests an antiferromagnetic Curie Weiss temperature of approximately -30 K. Below 10 K the temperature dependences of the inverse susceptibilities in the in-plane and perpendicular-to-plane directions are parallel, indicative of an isotropic magnetic moment at low temperatures. No sign of magnetic ordering is observed above 1.8 K, suggesting that ErMgGaO₄ is a geometrically frustrated magnet.

1. Introduction

Geometrically frustrated magnets are systems where the structure of the material hinders the appearance of long-range magnetic ordering on cooling to low temperatures¹⁻³. The simplest example is the case of antiferromagnetic interactions on an equilateral triangular lattice: as each corner is equidistant from the other two on such a lattice, there is no simple way to arrange magnetic spins such that they are purely antiparallel to their nearest neighbors. Thus the spins may fail to order down to temperatures below the Weiss temperature, and when ordering finally does occur it is frequently into a state that is a compromise between parallel and antiparallel spins¹⁻⁶.

The YbFe_2O_4 structure type is layered, with a single-layer equilateral triangular lattice of large-metal-oxygen octahedra sharing edges separated by a bilayer of M-O triangular bipyramids⁷. Compounds in this family exhibit a wide variety of unusual electronic and magnetic properties, including ferroelectricity⁸⁻¹¹, charge density waves^{9,12}, and spin glass behavior¹³⁻¹⁶. As the structure allows for many different kinds atoms to occupy each site, many compounds have been synthesized^{17,18}. Recently, the YbFe_2O_4 -type material YbMgGaO_4 has drawn attention as a potential quantum spin liquid candidate¹⁹⁻²⁴, inviting investigation of the properties of the most closely-related compounds in the family. Here we report the single-crystal growth and basic magnetic properties of ErMgGaO_4 , a compound whose crystal structure has been reported^{17,25} though we report in the following that one significant aspect of the structure was overlooked - the Er site disorder.

2. Materials and Methods

Small crystals of ErMgGaO_4 were synthesized via the floating zone method from a stoichiometric mixture of Er_2O_3 (99.99%, Alfa Aesar), Ga_2O_3 (99.999%, Alfa Aesar), and MgO (99.95%, Alfa Aesar). The powders were ground together in ethanol using an agate mortar and pestle and mixed with stearic acid in a 12:1 molar ratio. When dry, the powder was loaded into a rubber tube and hydrostatically compressed to 40 MPa. The resulting rod (8 cm long, 6 mm diameter) was heated at 1°C per minute to a temperature of 1200°C, heated for four hours, then cooled to room temperature. The rod was then

transferred to a four-mirror optical floating zone (FZ) furnace (Crystal Systems, Inc. Model No. FZ-T-10000-HVP-II-P) with 4 x 1500 W lamps. The rod was sintered in the FZ furnace at 50.0% output power with a rotation rate of 10 RPM and a rate of travel of 5 mm/hr. The sintered rod was then cut into lower and upper feed rods, and a crystal growth was performed at 54.1% output power, with a rotation rate of 12 RPM and a growth rate of 3 mm/hr. The resulting crystal growth displayed large, clear facets and had a red color, but was cloudy and translucent when viewed under a microscope, suggesting a high degree of either twinning or impurity phases. Small portions of the crystal facets were carefully removed from the rod, and determined to be clear platelike single crystals of ErMgGaO_4 . No pure crystals were obtained larger than 1 mm in largest dimension.

The crystal structure of ErMgGaO_4 was determined by single-crystal X-ray diffraction (SXRD), especially to test for possible positional disorder of Er and to evaluate the Ga/Mg mixed occupancy position. The SXRD data was collected at 296 K with a Bruker D8 VENTURE diffractometer equipped with a PHOTON CMOS detector using graphite-monochromatized $\text{Mo-K}\alpha$ radiation ($\lambda = 0.71073 \text{ \AA}$). The raw data was corrected for background, polarization, and the Lorentz factor using APEX3 software²⁶, and multi-scan absorption correction using the SADABS-2016/2 program package was applied²⁷. The structure was solved with the charge flipping method²⁸ and subsequent difference Fourier analyses with Jana2006²⁹⁻³⁰. Structure refinement against F_o^2 was performed with Shelxl-2017/1³¹⁻³². Additional room temperature measurements on single crystal plates lying on a glass slide were taken using a Bruker D8 Advance Eco diffractometer with $\text{Cu-K}\alpha$ radiation ($\lambda = 1.5418 \text{ \AA}$) and a LynxEye-XE detector.

Magnetic measurements were taken using a Quantum Design Physical Property Measurement System (PPMS) Dynacool with a vibrating sample mount. The temperature-dependent DC magnetization (M) was measured for a 1.1 mg ($\sim 1 \text{ mm} \times 0.2 \text{ mm}$) single crystal of ErMgGaO_4 from 1.8 K to 300 K. The magnetic susceptibility was defined as M/H , where H is the applied field in Oe.

Magnetization vs. applied field measurements in fields of up to 90 kOe were taken at 2 K and 15 K.

Both types of measurements were taken both parallel and perpendicular to the c -axis of the crystal. For measurements parallel to c , the crystal was placed in a plastic sample holder. For measurements perpendicular to c , the sample was mounted onto a silica sample holder with GE varnish.

3. Results and Discussion

3.1 Crystal Structure

The crystal structure of ErMgGaO_4 was determined from the refinement of single crystal XRD data and compared to previously published structure models^{17,25}; it can be seen in Figure 1.a.

ErMgGaO_4 crystallizes in the space group $R\bar{3}m$ (no. 166), with ambient temperature lattice parameters were determined to be $a = 3.4317(1)$ Å and $c = 25.104(1)$ Å. Although previous reports suggested that the Er atom sits directly on the high-symmetry $[0\ 0\ 0]$ site, the initial structure model with anisotropic refined thermal parameters for Er on this site (Wyckoff site $3a$, $[0\ 0\ 0]$) revealed an anomalously broad electron distribution along the z -axis. The examination of the Fourier (F_{obs}) map (Figure 1.b) revealed significantly elongated electron density maxima along z for the Er position, clearly reflecting the presence of positional disorder of the rare earth metal. An appropriate displaced site (Wyckoff site $6c$, with a free parameter allowing the displacement of the Er along c) was therefore introduced to describe the statistical positional disorder of the rare earth atom. The refined positional displacement of the Er from $[0,0,0]$ was highly significant, at about 60 standard deviations, with coordinates refined to $[0, 0, 0.00418(7)]$. 50% occupancy was used for each of these Er sites because the resulting Er positions are separated by $2 \times 0.00418 \times 25.1$ Å = 0.21 Å and are therefore too close to be simultaneously occupied. This position for the rare earth atom, displaced along c , is consistent with the published structures of several related compounds¹³. The disorder for the rare earth atom positions in the related materials YbMgGaO_4 ²² and TmMgGaO_4 ³³ has previously been attributed to the disorder in the local environment caused by the random mixing of Mg and Ga atoms in the neighbouring layers. As is generally the case

for mixed atom occupancy positions, the displacement parameters and the coordinates for the Ga and Mg atoms were constrained to be equal in our structural refinement of ErMgGaO₄. The final atomic parameters are summarized in Table 1, and further crystallographic data can be seen in the supplementary information (Supplementary Tables 1 and 2).

3.2 Magnetism

A platelike single crystal of ErMgGaO₄ was isolated from the crystal growth, placed on a glass slide, and analyzed on the powder X-ray diffractometer in the flat plate geometry. This XRD scan showed only peaks corresponding to the (00*l*) planes in the ErMgGaO₄ crystal structure, indicating that the large face of the crystal was orthogonal to the *c*-axis. This X-ray pattern, as well as a photo of the thus characterized crystal used in the diffraction and magnetization measurements can be seen in Figure 1.c.

The temperature-dependent magnetic susceptibility of single crystal ErMgGaO₄, measured parallel and perpendicular to the *c*-axis in a field of 10 kOe, is shown in Figure 2. The susceptibility was fit to the Curie-Weiss Law, $\chi - \chi_0 = C / (T - \theta_w)$, where χ is the susceptibility, C is the Curie Constant, θ_w is the Weiss temperature, and χ_0 is a temperature-independent contribution. This contribution was determined to be -0.004 emu mol⁻¹ parallel to *c*, and -0.0055 emu mol⁻¹ perpendicular to *c*, values that include the contributions from the sample holder and are therefore not considered precise. The resulting values for the Curie-Weiss fits at high temperature (150-300 K) and low temperature (2-10 K) are summarized in Table 2. For measurements parallel to *c* at high temperature, θ_w was determined to be -51.9 K, and C was determined to be 14.21. The effective magnetic moment (μ_{eff}) was determined by the equation $\mu_{\text{eff}} = \sqrt{8C}$, and was found to be 10.7 μ_B . Perpendicular to *c*, high-temperature measurements produced values for θ_w of -18.4 K, C of 8.68, and an effective magnetic moment of 8.3 μ_B , suggesting a degree of magnetic anisotropy that is likely due to the material's layered structure. The negative Weiss temperatures are indicative of dominantly antiferromagnetic exchange interactions, but

the susceptibility curves themselves show no indication of magnetic ordering transitions down to 1.8 K. This suggests that ErMgGaO₄ is a material that exhibits a significant degree of geometric magnetic frustration, much like the related materials TmMgGaO₄³³ and YbMgGaO₄¹⁹.

At lower temperatures, the susceptibilities show a notable deviation from ideal Curie-Weiss behavior. The inverse susceptibility curves of the two orientations cross near 20 K, and below 10 K they are almost parallel. Curie-Weiss fits in this low temperature region resulted in values of $C = 5.75$, $\theta_W = -7.5$ K, and $\mu_{\text{eff}} = 6.8 \mu_B$ parallel to c , and values of $C = 6.12$, $\theta_W = -5.3$ K, and $\mu_{\text{eff}} = 7.0 \mu_B$ perpendicular to c .

Field-dependent magnetization was measured along both orientations at 2 K, the results of which can be seen in the inset of Figure 2. The measurement parallel to c showed a linear magnetic response up to approximately $\mu_0 H = 2$ Tesla, although M vs. H curves significantly at higher fields, not showing a tendency towards saturation below $\mu_0 H = 9$ Tesla. Perpendicular to c , the magnetization curve shows again shows linearity up to fields of approximately $\mu_0 H = 2$ Tesla, but then shows a greater tendency towards saturation, although saturation is not reached by $\mu_0 H = 9$ Tesla. The magnetization observed near $\mu_0 H = 9$ Tesla is significantly less than what is expected if all the Er moments are oriented along the magnetic field direction. From the magnetic data it can be concluded that ErMgGaO₄ exhibits a degree of magnetic anisotropy, although the effect is much weaker than in the closely related system TmMgGaO₄³³ and is closer in magnitude to what is observed in YbMgGaO₄ and YbZnGaO₄³⁴.

The individual single crystals of ErMgGaO₄ used for the diffraction and magnetization measurements were identified via the use of the X-ray Diffractometer in flat plate geometry to look at the out-of-plane X-ray scattering, as described above. The mixing of such crystals with impurity phases such as the Er₃Ga₅O₁₂ garnet in the floating zone growth rod made it impractical to isolate a bulk powder sample for magnetic characterization, and thus we estimate the average magnetic behavior by taking the averages of the directional measurements on the single crystal (2/3 of the susceptibility perpendicular to c , and 1/3 of the susceptibility parallel to c). The resulting curve is plotted in Figure 3.

A high-temperature (150-300 K) Curie-Weiss fit of this average curve yielded values of $C = 10.49$, $\theta_W = -30.4$, and $\mu_{\text{eff}} = 9.2 \mu_B$. This value for the effective magnetic moment is close to the ideal of $9.59 \mu_B$ per Er expected for a free ion. At low temperatures, the average curve is nearly parallel to the two directional measurements, as expected from the direction-dependent data. A Curie-Weiss fit to the region between 2 K and 10 K yielded values of $C = 6.01$, $\theta_W = -5.9$, and $\mu_{\text{eff}} = 6.9 \mu_B$. A temperature-dependent magnetization measurement in the low temperature region in an applied field of 1 kOe is displayed in the rightmost inset in Figure 3, and shows that in this lower field, there is also no evidence of magnetic ordering in the magnetic susceptibility down to temperatures of 1.8 K.

4. Conclusions

Small single crystals of the equilateral triangular plane lattice material ErMgGaO_4 have been synthesized via the optical floating zone method, and the structure has been determined using single-crystal X-ray diffraction. The lattice parameters and atomic positions are generally found to be in good agreement with previously published values for this and other isostructural compounds. Notably, however, the magnetic Er ions are in disordered positions, a consideration that is important when modeling the magnetic behavior. Magnetic measurements suggest that the magnetism in the material is dominated by antiferromagnetic interactions, although no magnetic ordering is observed above 1.8 K, suggesting the presence of geometric magnetic frustration. Some anisotropy is observed in the magnetic measurements, in line with related compounds in this structure type and consistent with the layered structure of the material.

Continued work on the synthesis of this material is warranted. A pure powder sample may be of interest for initial characterization of the magnetic system by neutron diffraction. Additionally, this material and its family of related compounds is worthy of further study due to its combination of an isolated, equilateral triangular plane lattice of spins plus subtle structural distortions of that lattice caused by local disorder in non-magnetic ions in the adjacent planes. Finally, the growth of larger single crystals for detailed neutron scattering measurements may provide valuable insight into these

compounds, and warrants further effort.

Acknowledgments

This research was supported by the US Department of Energy, Division of Basic Energy Sciences, Grant No. DE-FG02-08ER46544, and was performed under the auspices of the Institute for Quantum Matter.

References

1. Lacroix, C., Mendels, P., Mila, F., *Introduction to Frustrated Magnetism* (Springer-Verlag Berlin Heidelberg, 2011).
2. Diep, H. T. *et al.*, *Frustrated Spin Systems* (World Scientific Publishing Co., Singapore, 2004).
3. Sadoc, J. F., Mosseri, R., *Geometrical Frustration* (Cambridge University Press, Cambridge, 1999).
4. Ramirez, A. P., *Annu. Rev. Mater. Sci.*, **24**, 453-480 (1994).
5. Balents, L., *Nature*, **464** (2010).
6. Gardner, J. A., Gingras, M. J. P., Greedan, J. E., *Rev. Mod. Phys.*, **82** (53), (2010).
7. Kato, K., Kawada, I., Kimizuka, N., Katsura, T., *Zeit. Für Krist.*, **141**, 314-320 (1975).
8. Nagata, T., Janolin, P.-E., Fukunaga, M., Roman, B., Fujiwara, K., Kimura, H., Kiat, J.-M., Ikeda, N. *Appl. Phys. Lett.* **110**, 052901 (2017).
9. Hearmon, A. J., Prabhakaran, D., Nowell, H., Fabrizi, F., Gutmann, M. J., Radaelli, P. G., *Phys. Rev. B*, **85**, 014115 (2012).
10. Liu, Y., Zou, T., Wang, F., Zhang, X., Cheng, Z., Sun, Y. *Physica B. Cond. Mat.*, **405** (16), 3391-3394 (2010).
11. Ikeda, N. *J. of Phys. Cond. Mat.* **20** (43), (2008).
12. Zhang, Y., Yang, H. X., Guo, Y. Q., Ma, C., Tian, H. F., Luo, J. L., Li, J. Q., *Phys. Rev. B*, **76**, 184105 (2007).
13. Cava, R.J., Ramirez, A.P., Huang, Q., Krajewski, J.J. *J. Solid State Chem.* **140** (2), 337-344 (1998).
14. Fritsch, K., Ross, K. A., Granroth, G. E., Ehlers, G., Noad, H. M. L., Dabkowska, H. A., Gaulin, B. D., *Phys. Rev. B*, **96**, 094414 (2017).
15. Dabkowska, H. A., Dabkowska, A., Luke, G. M., Gaulin, B. D., *J. Crys. Growth*, **234** (2-3), 411-414 (2002).
16. Iida, J., Tanaka, M., Nakagawa, Y., *J. Phys. Soc. Jpn.*, **59**, 4443-4448 (1990).
17. Beznosikov, B. V. and Aleksandrov, K. S. *Krasnoyarsk*. Pre-print (2006).
18. Kimizuka, N., and Mohri, T. *J. Solid State Chem.* **60** (3), 382-384 (1985).
19. Li, Y., Chen, G., Tong, W., Pi, L., Liu, J., Yang, Z., Wang, X., Zhang, Q. *Phys. Rev. Lett.* **115**, 167203 (2015).
20. Paddison, J. A. M., Daum, M., Dun, Z. L., Ehlers, G., Liu, Y., Stone, M. B., Zhou, H. D., Mourigal, M. *Nature Physics* **13**, 177-122 (2017).

21. Li, Y., Adroja, D., Bewley, R., Voneshen, D., Tsirlin, A., Gegenwart, P., Zhang, Q. *Phys. Rev. Lett.* **118**, 107202 (2017).
22. Li, Y., Liao, H., Zhang, Z., Li, S., Jin, F., Ling, L., Zhang, L., Zou, Y., Pi, L., Yang, Z., Wang, J., Wu, Z., Zhang, Q. *Sci. Reports*, **5**, 16419 (2015).
23. Shen, Y., Li, Y.-D., Wo, H., Li, Y., Shen, S., Pan, B., Wang, Q., Walker, H. C., Steffens, P., Boehm, M., Hao, Y., Quintero-Castro, D. L., Harriger, L. W., Frontzek, M. D., Hao, L., Meng, S., Chang, Q., Chen, G., Zhao, J., *Nature*, **540**, 559-562 (2016).
24. Zhu, Z., Maksimov, P. A., White, S. R., Chernyshev, A. L., *Phys. Rev. Lett.*, **119**, 157201 (2017).
25. Kimizuka N., and Takayama, E. *J. Solid State Chem.* **41**, 166-173 (1982).
26. APEX3, Version v2017.3-0, Bruker AXS Inc., Madison, Wisconsin, USA, 2017.
27. Krause, L., Herbst-Irmer, R., Sheldrick, G. M., Stalke, D. *J. Appl. Cryst.* **48**, 3-10 (2015).
28. Oszlányi, G., Sütő, A. *Acta Crystallogr. A* **60**, 134 (2004).
29. Oszlányi, G., Sütő, A. *Acta Crystallogr. A* **64**, 123 (2008).
30. Petricek, V., Dusek, M., Palatinus, L. *Zeit. Kristallogr.* **229**, 345 (2014).
31. Sheldrick, G. M. *SHELX2017, Programs for crystal structure determination*, Universität Göttingen, Germany, 2017.
32. Sheldrick, G. M., *Acta Crystallogr. A*, **64**, 112 (2008).
33. Cevallos, F. A., Stolze, K., Kong, T., Cava, R. J. *Pre-print*. arXiv:1710.07707v1 (2017).
34. Ma, Z., Wang, J., Dong, Z., Zhang, J., Li, S., Zheng, S., Yu., Y., Wang, W., Che, L., Ran, K., Bao, S., Cai, Z., Cermak, P., Schneidewind, A., Yano, S., Gardner, J. S., Lu, X., Yu, S., Liu, J., Li, S., Li, J., Wen, J. *Phys. Rev. Lett.* **120**, 087201 (2018).

Table 1. Wyckoff positions, coordinates, occupancies, and equivalent isotropic displacement parameters respectively for an ErMgGaO₄ single-crystal measured at 296(1) K. $a = 3.4317(1)$ Å, $c = 25.104(1)$ Å. The coordinates and thermal parameters of Ga and Mg were constrained to be equal; U_{eq} is one third of the trace of the orthogonalized U_{ij} tensor.

Atom	Wyck. Site	x	y	z	Occupancy	$U_{\text{eq}}/U_{\text{iso}}$
Er	6c	0	0	0.00418(7)	0.5	0.00721(18)
Ga	6c	0	0	0.21406(2)	0.5	0.00484(5)
Mg	6c	0	0	0.21406(2)	0.5	0.00484(5)
O1	6c	0	0	0.29068(6)	1	0.00751(17)
O2	6c	0	0	0.12908(7)	1	0.0131(2)

Table 2. Magnetic properties of ErMgGaO₄, as determined from magnetization vs. temperature measurements parallel and perpendicular to the c -axis in an applied field of 10 kOe.

Direction	Region of M-T curve	Curie Constant (C)	Weiss Temperature (θ_w)	Effective Magnetic Moment (μ_{eff})
Parallel to c	High-T	14.21	-51.9 K	10.7 μ_B
	Low-T	5.75	-7.5 K	6.8 μ_B
Perpendicular to c	High-T	8.68	-18.4 K	8.3 μ_B
	Low-T	6.12	-5.3 K	7.0 μ_B
Weighted average	High-T	10.49	-30.4 K	9.2 μ_B
	Low-T	6.01	-5.9 K	6.9 μ_B

Figure captions

Figure 1. (a) The crystal structure of ErMgGaO₄ showing the coordination polyhedra. ErO₆ octahedra are olive, Mg/GaO₅ triangular bipyramids are green. On the right is the triangular arrangement of Er atoms as viewed down the *c*-axis. In the bottom right is a closer view of the distorted ErO₆ octahedra and the slightly off-center nature of the Er positions. (b) F_{obs} Fourier map for ErMgGaO₄ based on room-temperature data; in space group $R\bar{3}m$, map is sum of electron density between $-0.10 < y < 0.10$, contour lines correspond to $12 \text{ e}/\text{\AA}^3$. (c) X-ray diffraction pattern of a single crystal of ErMgGaO₄, showing only peaks corresponding to (00*l*) planes. Inset: A picture of the actual crystal used in measurements.

Figure 2. Temperature-dependent magnetic susceptibility of ErMgGaO₄ measured parallel (blue) and perpendicular (red) to the *c*-axis in an applied field of 10 kOe. Inset: The field-dependent magnetization of ErMgGaO₄ measured parallel and perpendicular to the *c*-axis at a temperature of 2 K.

Figure 3. Temperature-dependent inverse susceptibility curves of ErMgGaO₄ measured parallel (blue) and perpendicular (red) to the *c*-axis in an applied field of 10 kOe. In pink is the weighted average of the two curves (2/3 perpendicular, 1/3 parallel). Left inset: The low-temperature region of the temperature-dependent inverse susceptibility curves. Right inset: The low-temperature region of the temperature-dependent susceptibility curves measured in an applied field of 1 kOe.

Figures

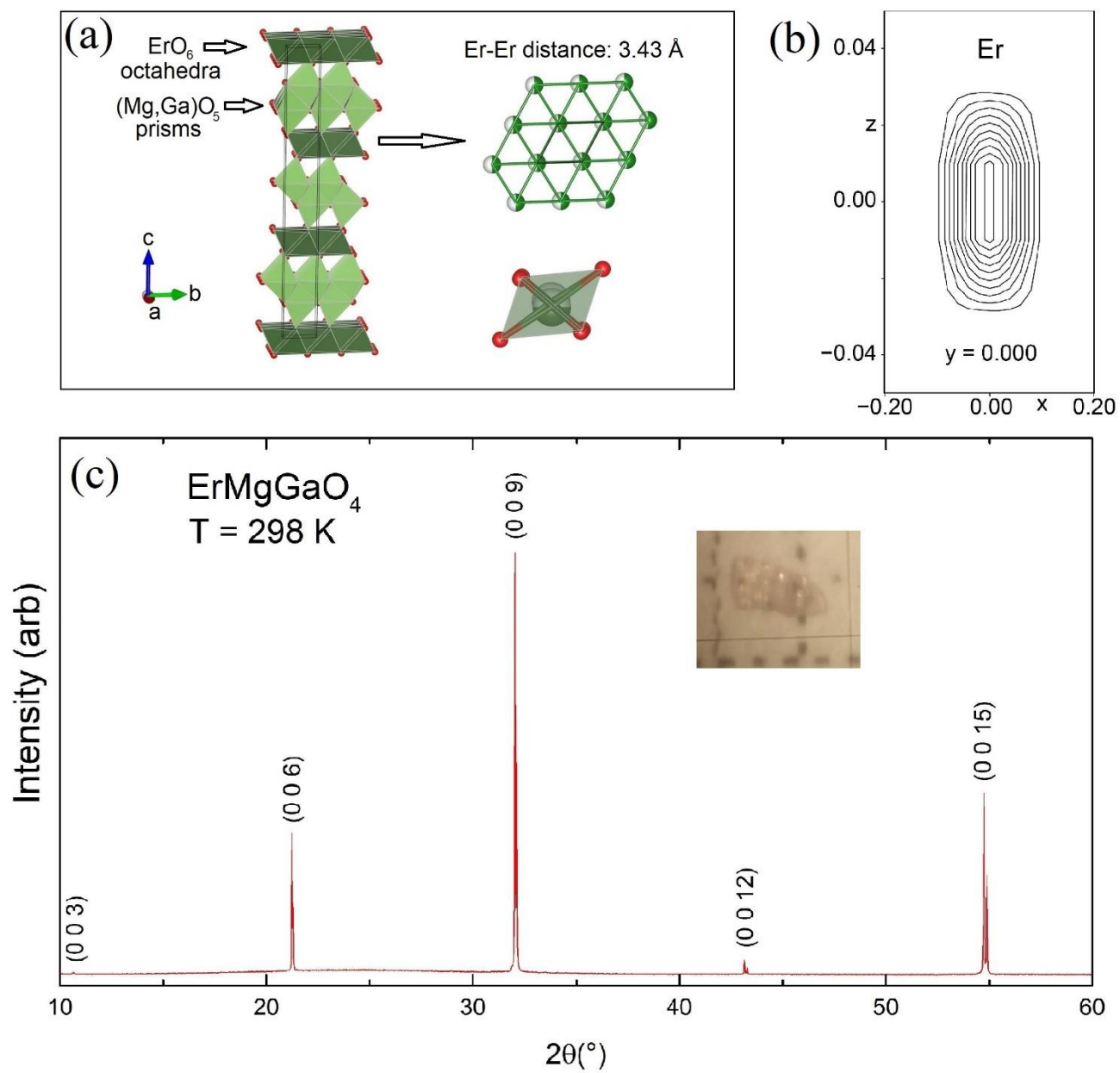


Figure 1

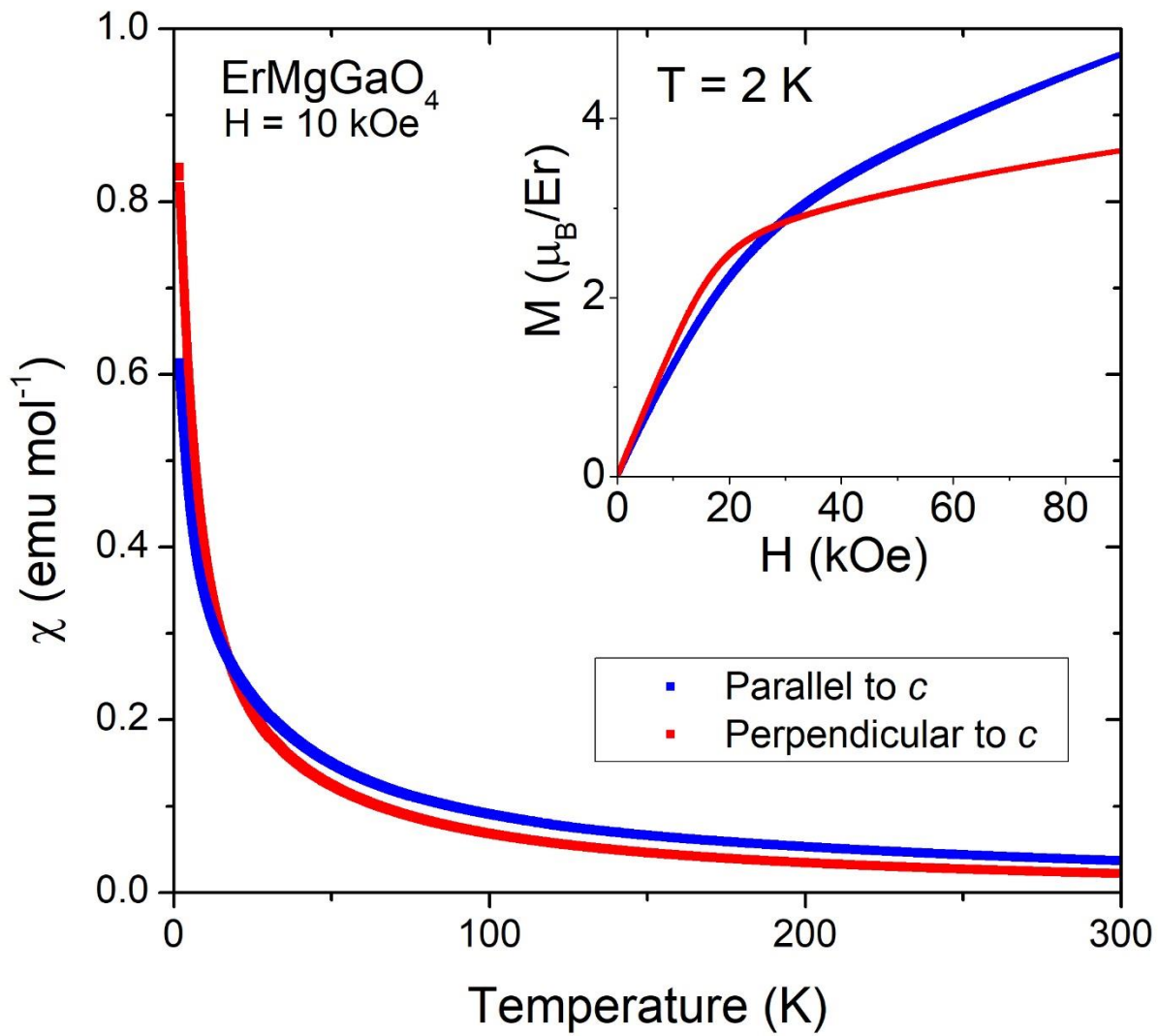


Figure 2

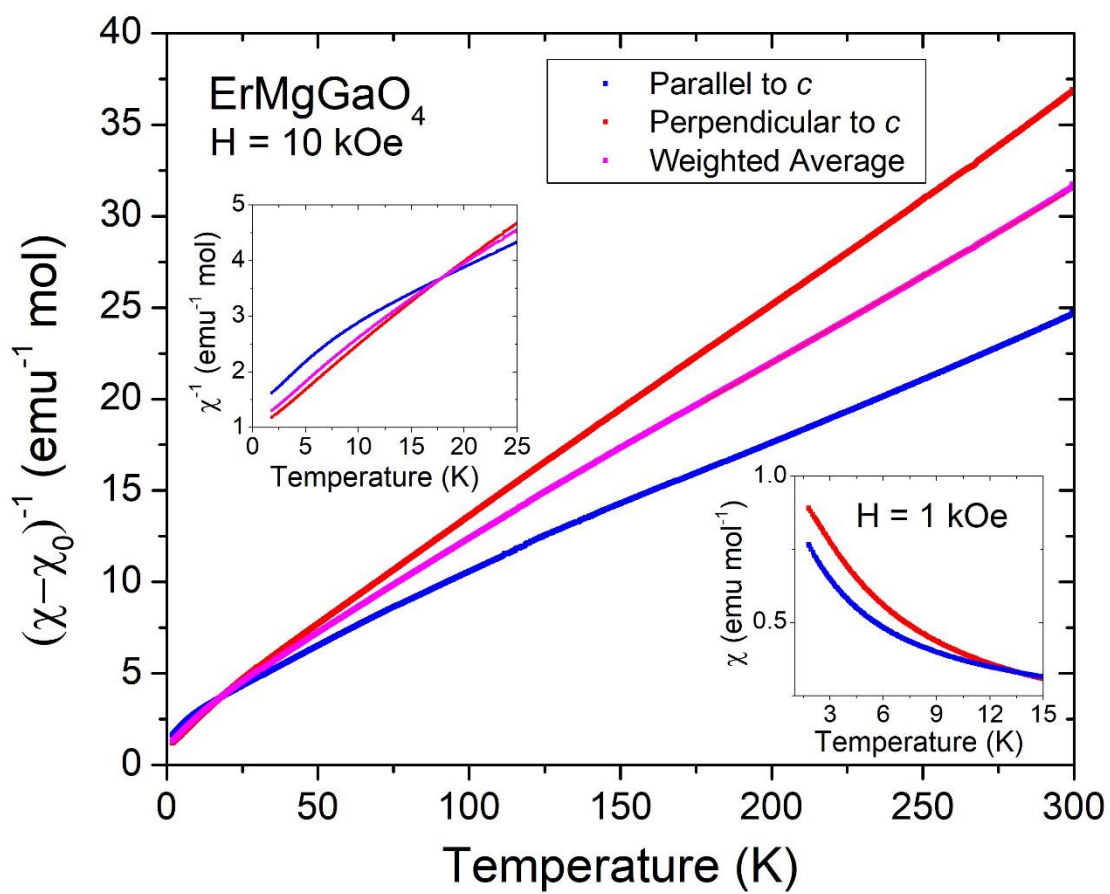


Figure 3

Supplementary Information

Supplementary Table 1. Crystallographic data and details of the structure determination of ErMgGaO₄ derived from single-crystal experiments measured at 296(1) K.

Sum Formula	ErMgGaO ₄
Formula weight / (g · mol ⁻¹)	325.29
Crystal System	trigonal
Space group	<i>R</i> -3 <i>m</i> (no. 166)
Formula units per cell, <i>Z</i>	3
Lattice parameter <i>a</i> / Å	3.4317(1)
<i>c</i> / Å	25.104(1)
Cell volume / (Å ³)	256.03(2)
Calculated density / (g · cm ⁻³)	6.329
Radiation	$\lambda(\text{Mo-}K\alpha) = 0.71073 \text{ \AA}$ $2\theta \leq 95.66^\circ$
Data range	$-7 \leq h \leq 7$ $-7 \leq k \leq 7$ $-50 \leq l \leq 51$
Absorption coefficient / mm ⁻¹	32.33
Measured reflections	6738
Independent reflections	362
Reflections with $I > 2\sigma(I)$	345
<i>R</i> (int)	0.036
<i>R</i> (σ)	0.013
No. of parameters	12
<i>R</i> ₁ (obs)	0.011
<i>R</i> ₁ (all <i>F</i> _o)	0.012
<i>wR</i> ₂ (all <i>F</i> _o)	0.023
Residual electron density / (e · Å ⁻³)	0.95 to -0.94

Supplementary Table 2. Anisotropic thermal displacement parameters for ErMgGaO₄ single-crystal measured at 296(1) K. The coefficients U_{ij} (\AA^2) of the tensor of the anisotropic temperature factor of atoms are defined by $\exp\{-2\pi^2[U_{11}h^2a^{*2} + \dots + 2U_{23}k lb^* c^*]\}$; $U_{ij}[\text{Ga}]$ and $U_{ij}[\text{Mg}]$ were constrained to be equal.

Atom	U_{11}	U_{22}	U_{33}	U_{12}
Er	0.00290(4)	0.00290(4)	0.0158(5)	0.00145(2)
Ga/Mg	0.00448(6)	0.00448(6)	0.00557(12)	0.00224(3)